Tissue-Specific Control of the Endocycle by the Anaphase Promoting Complex/Cyclosome Inhibitors UVI4 and DEL1[1][OPEN]

Jefri Heyman, Stefanie Polyn, Thomas Eekhout, and Lieven De Veylder[2]

Department of Plant Biotechnology and Bioinformatics, Ghent University, 9052 Ghent, Belgium and Center for Plant Systems Biology, VIB, 9052 Ghent, Belgium

ORCID IDs: 0000-0003-3266-4189 (J.H.); 0000-0002-7847-6506 (S.P.); 0000-0002-2878-1553 (T.E.); 0000-0003-1150-4426 (L.D.V.).

The endocycle represents a modified mitotic cell cycle that in plants is often coupled to cell enlargement and differentiation. Endocycle onset is controlled by activity of the Anaphase Promoting Complex/Cyclosome (APC/C), a multisubunit E3 ubiquitin ligase targeting cell-cycle factors for destruction. CELL CYCLE SWITCH52 (CCS52) proteins represent rate-limiting activator subunits of the APC/C. In Arabidopsis (*Arabidopsis thaliana*), mutations in either *CCS52A1* or *CCS52A2* activators result in a delayed endocycle onset, whereas their overexpression triggers increased DNA ploidy levels. Here, the relative contribution of the APC/$C^{CCS52A1}$ and APC/$C^{CCS52A2}$ complexes to different developmental processes was studied through analysis of their negative regulators, being the ULTRAVIOLET-B-INSENSITIVE4 protein and the DP-E2F-Like1 transcriptional repressor, respectively. Our data illustrate cooperative activity of the APC/$C^{CCS52A1}$ and APC/$C^{CCS52A2}$ complexes during root and trichome development, but functional interdependency during leaf development. Furthermore, we found APC/$C^{CCS52A1}$ activity to control *CCS52A2* expression. We conclude that interdependency of CCS52A-controlled APC/C activity is controlled in a tissue-specific manner.

The endocycle represents a modified version of the mitotic cell cycle during which the genome is replicated in the absence of mitosis and cytokinesis, resulting in a doubling of the nuclear DNA content (De Veylder et al., 2011; Edgar at al., 2014). Endoreplication is a common feature among eukaryotes, frequently observed in cell types with a high metabolic activity (Larkins et al., 2001). In *Drosophila melanogaster*, endoreplication is predominantly seen in larval tissues and the salivary glands (Lilly and Duronio, 2005), whereas in *Caenorhabditis elegans*, it is observed in the syncytium (Flemming et al., 2000). In higher plants, like Arabidopsis (*Arabidopsis thaliana*), endoreplication is observed in most tissues and is coupled to cell differentiation (Breuer et al., 2010), such as in developing leaves, where the onset of the endocycle marks the exit from cell division (Beemster et al., 2006). Furthermore, endoreplication is believed to be an important trigger for cell and organ growth, because cell size is frequently correlated with the DNA ploidy levels (Melaragno et al., 1993; De Veylder et al., 2011), although such a relationship is not always observed (Beemster et al., 2002). In tomato (*Solanum lycopersicum*), increased ploidy levels are correlated with increased levels of rRNA and protein synthesis per-nucleus, indicating increased metabolism to support cell growth (Bourdon et al., 2012). Endoreplication has also been demonstrated to instruct cell fate, as observed for Arabidopsis trichomes (Bramsiepe et al., 2010). More recently, endocycle modulators have been implicated in the control of innate immunity in Arabidopsis (Hamdoun et al., 2016), suggestive for the importance of the endocycle in the plant immunity.

In all eukaryotes, control of the mitotic cell cycle, cell differentiation, and endocycle onset is achieved by the Anaphase Promoting Complex/Cyclosome (APC/C). The APC/C is a conserved E3 ubiquitin ligase that ubiquitinates key cell cycle proteins containing APC/C recognition motifs known as the Destruction or KEN/GxEN-boxes, resulting in their destruction by the proteasome, thereby ensuring the unidirectional cell cycle progression (Heyman and De Veylder, 2012). During the late G2 and early M phase, the APC/C is activated by the CDC20/Fizzy activator subunit, which itself is targeted for destruction during the anaphase and substituted by the CDH1/FZR type activator subunit, known in plants as CELL CYCLE SWITCH52 (CCS52) proteins (Peters,

[1] This work was supported by grants of the Research Foundation Flanders (G.023616N) and the Interuniversity Attraction Poles Programme (IUAP P7/29 "MARS"), initiated by the Belgian Science Policy Office. J.H. and S.P. are indebted to the Research Foundation-Flanders for a post- and is a predoctoral Fellowship, respectively. T.E. is supported by the Agency for Innovation by Science and Technology in Flanders for a predoctoral fellowship.

[2] Address correspondence to lieven.deveylder@ugent.vib.be.

The author responsible for distribution of materials integral to the findings presented in this article in accordance with the policy described in the Instructions for Authors (www.plantphysiol.org) is: Lieven De Veylder (lieven.deveylder@ugent.vib.be).

J.H. and L.D.V. conceived and designed the experiments; J.H., S.P., and T.E. performed the experiments; J.H. and L.D.V. analyzed the data; J.H. and L.D.V. wrote the manuscript.

[OPEN]Articles can be viewed without a subscription.

www.plantphysiol.org/cgi/doi/10.1104/pp.17.00785

2002; Baker et al., 2007). The Arabidopsis genome encodes two types of CCS52 proteins, namely the A-type, consisting of CCS52A1 and CCS52A2, and B-type CCS52B (Cebolla et al., 1999). Whereas the function of CCS52B in the cell cycle is still unclear, both CCS52A1 and CCS52A2 activator subunits have been demonstrated to control endocycle onset (Cebolla et al., 1999; Lammens et al., 2008; Narbonne-Reveau et al., 2008; Mathieu-Rivet et al., 2010). In the Arabidopsis root, APC/$C^{CCS52A1}$ activity controls the timing of endocycle onset by marking the A-type cyclin CYCA2;3 for destruction (Imai et al., 2006; Boudolf et al., 2009). Correspondingly, *ccs52a1* mutants display roots with an expanded meristem size owing to an increased number of meristematic cells (Vanstraelen et al., 2009). CCS52A1 also drives the trichome endocycle and trichome branching, as *ccs52a1* loss-of-function mutant trichomes display two branches in contrast to wild-type trichomes that predominantly contain three branches. Correspondingly, *CCS52A1* overexpression results in trichome overbranching (Imai et al., 2006; Kasili et al., 2010). In contrast to CCS52A1, the CCS52A2 activator subunit appears not to control root meristem size, but is instead required for stem cell maintenance by suppressing cell division of the Quiescent Center (QC) stem cells, as *ccs52a2* mutants display increased QC cell division rates being correlated with a disorganization of the root meristem (Vanstraelen et al., 2009). CCS52A2 might play a similar role in the shoot, as its absence results in a disrupted cell organization of the L1 and L2 layers (Liu et al., 2012). In leaves, both CCS52A1- and CCS52A2-activated APC/C complexes control endocycle onset, as mutation of either results in reduced DNA ploidy levels (Lammens et al., 2008). Functional redundancy between CCS52A1 and CCS52A2 is additionally suggested by the observation that no viable double mutant plants can be obtained (Baloban et al., 2013).

Due to its importance during development, APC/C^{CCS52A} activity is tightly controlled at both the transcriptional and posttranslational levels. On the transcriptional level, expression of both *CCS52A1* and *CCS52A2* is negatively regulated by E2Fa in complex with RETINOBLASTOMA-RELATED PROTEIN1 (RBR1). Overexpression of a mutated *E2Fa* allele, lacking the RBR1 interaction domain, results in increased *CCS52A* expression, indicating that recruitment of RBR1 is required to suppress gene expression (Magyar et al., 2012). *CCS52A1* expression is additionally negatively regulated by the GT2-LIKE1 trihelix transcription factor (Breuer et al., 2012), whereas its transcription is activated by the cytokinin-activated ARABIDOPSIS RESPONSE REGULATOR2 (Takahashi et al., 2013). *CCS52A2* expression rather appears to be specifically repressed by the atypical E2F transcription factor DEL1, which acts as a negative regulator of endocycle onset (Vlieghe et al., 2005; Lammens et al., 2008). Mutation of *DEL1* results in increased *CCS52A2* expression and APC/$C^{CCS52A2}$ activity, resulting in a premature endocycle onset and increased DNA ploidy levels. At the posttranslational level, the UVI4 protein, in association with the UBIQUITIN-SPECIFIC PROTEASE14, has been found to be an inhibitor of the APC/$C^{CCS52A1}$ complex (Heyman et al., 2011; Xu et al., 2016). Double mutant analysis of plants lacking a functional *CCS52A1* and *UVI4* gene revealed that CCS52A1 functions epistatically over UVI4 in controlling endocycle onset. Correspondingly, UVI4 regulates endocycle onset in leaves and root meristem size maintenance by inhibiting APC/$C^{CCS52A1}$ activity, as observed by the increased DNA ploidy levels in leaves and trichomes, and a reduced number of meristematic cells in the root tip of *uvi4* mutant plants (Hase et al., 2006; Heyman et al., 2011). Here we aimed to study the interplay and specificity of APC/$C^{CCS52A1}$ and APC/$C^{CCS52A2}$ during plant development. For this purpose, we performed a comparative phenotypic analysis of their negative regulators, being UVI4 and DEL1, respectively, as such circumventing the artificial and unspecific effects that might result from constitutive *CCS52A1* and *CCS52A2* overexpression.

RESULTS

CCS52A Activators Are Indispensable for Plant Development

Because of the importance of the CCS52A proteins in cell cycle exit and endocycle onset, we aimed to test the effects of deficiency in both *CCS52A1* and *CCS52A2* during plant development. Because *ccs52a1-1 ccs52a2-1* double mutants are not viable (Vanstraelen et al., 2009; Baloban et al., 2013), we generated a *ccs52a1-1 DEL1^{OE}* double mutant, which lacks a functional *CCS52A1* and displays reduced *CCS52A2* expression, owing to increased activity of the DEL1 transcriptional repressor (Lammens et al., 2008). Using flow cytometry, we confirmed the previously observed reduced DNA ploidy levels of the *ccs52a1-1* and *DEL1^{OE}* single mutant leaves compared to the wild type (Vlieghe et al., 2005; Vanstraelen et al., 2009; Baloban et al., 2013; Fig. 1A; Supplemental Table S1). In *ccs52a1-1 DEL1^{OE}* double mutant leaves, an additional decrease in the DNA ploidy level compared to those of the single mutants could be observed (Fig. 1A; Supplemental Table S1), confirming that expression of both *CCS52A* genes contribute to endocycle onset in the leaf.

Independently, the trichome branch number was quantified, which frequently correlates with the DNA content (Perazza et al., 1999a). Whereas the *ccs52a1-1* mutant plants display trichomes with a reduced number of branches, the *DEL1^{OE}* trichome branch number did not differ from that of the wild type, but the *ccs52a1-1 DEL1^{OE}* double mutant showed a trichome branch number similar to that of the *ccs52a1-1* mutant (Fig. 1B; Supplemental Fig. S1A). In addition, the trichome nuclear size was investigated. Corresponding to the reduced trichome branch number, a reduction in trichome nuclear size of the *ccs52a1-1* mutant was observed (Fig. 1C; Supplemental Fig. S1B), confirming previous findings (Heyman et al., 2011). Whereas no difference in trichome nuclear size of the *DEL1^{OE}* mutant could be detected, the *ccs52a1-1 DEL1^{OE}* double mutant displayed a reduced

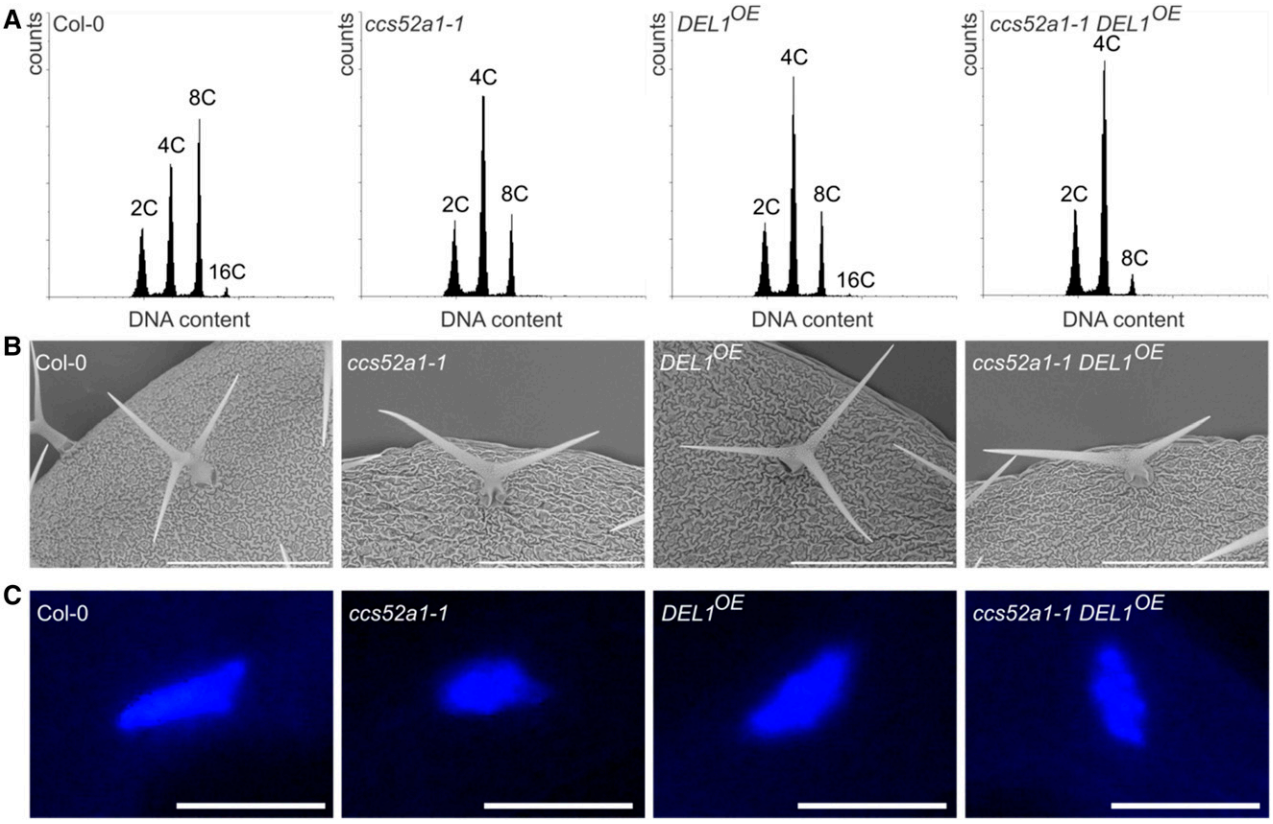

Figure 1. Endoreplication phenotypes of the *ccs52a1-1 DEL1*^{OE} double mutant. A, Flow cytometric analysis of wild-type (Col-0), *ccs52a1-1*, *DEL1*^{OE}, and *ccs52a1-1 DEL1*^{OE} three-week-old first true leaves. Data are representative for the mean (n = 3). B, Scanning electron microscope images of wild-type (Col-0), *ccs52a1-1*, *DEL1*^{OE}, and *ccs52a1-1 DEL1*^{OE} trichomes. Images are representative for the mean (n = 3). Bars = 300 μm. C, Epifluorescence images of DAPI-stained wild-type, *ccs52a1-1*, *DEL1*^{OE}, and *ccs52a1-1 DEL1*^{OE} trichome nuclei. Images are representative for the mean ($n > 13$). Bars = 10 μm.

nuclear size, comparable to that of the *ccs52a1-1* single mutant (Fig. 1C; Supplemental Fig. S1B), confirming previous data that CCS52A1 is the main APC/C activator in trichomes.

UVI4 Is a Specific Inhibitor of CCS52A1

Previously, we demonstrated that UVI4 acts as an inhibitor of APC/C^{CCS52A1} (Heyman et al., 2011). Using leaf ploidy levels, and trichome nuclear size and branching phenotype as a readout, the *ccs52a1-1* mutation was found to be epistatic over *uvi4* (Heyman et al., 2011). To test whether a similar genetic relationship exists between CCS52A2 and UVI4, the leaf ploidy level and trichome nuclear size of the *uvi4 ccs52a2-1* double mutant was compared with that of the single mutants. Whereas the *uvi4* and *ccs52a2-1* single mutants showed an increase and decrease in DNA ploidy levels compared to the wild type, respectively, the *uvi4 ccs52a2-1* double mutant contained DNA ploidy levels intermediate to those of the single mutants (Fig. 2A; Supplemental Table S2). Additionally, the trichome branch number was quantified. As demonstrated previously, *uvi4* mutants display increased trichome branching (Perazza et al., 1999b; Hase et al., 2006; Heyman et al., 2011), whereas the *ccs52a2-1* mutant showed a mild reduction in the number of trichomes containing four branches compared to the wild type (Fig. 2B; Supplemental Fig. S2A), correlating with trichome nuclear size (Fig. 2C and Supplemental Fig. S2B). The *uvi4 ccs52a2-1* double mutant displayed a trichome branch number intermediate to that of the *uvi4* and *ccs52a2-1* single mutants, again corresponding to the observed nuclear size (Fig. 2, B and C; Supplemental Fig. S2B). Combined with the previously observed protein-protein interaction of UVI4 with CCS52A1 but not CCS52A2 (Heyman et al., 2011), these data suggest that UVI4 is a specific inhibitor of APC/C^{CCS52A1}.

UVI4 and *DEL1* Are Coexpressed in Arabidopsis Seedlings

To investigate the putative interplay between UVI4 and DEL1 during plant development, we compared their expression patterns using transcriptional *GUS* reporter lines. Expression of both *UVI4* and *DEL1* could be detected in tissues showing a high cell division activity, such as the root meristem (Fig. 3A) and shoot meristem, and young leaves (Fig. 3B). Thus it appears that both APC/C regulators are tightly coexpressed, suggesting

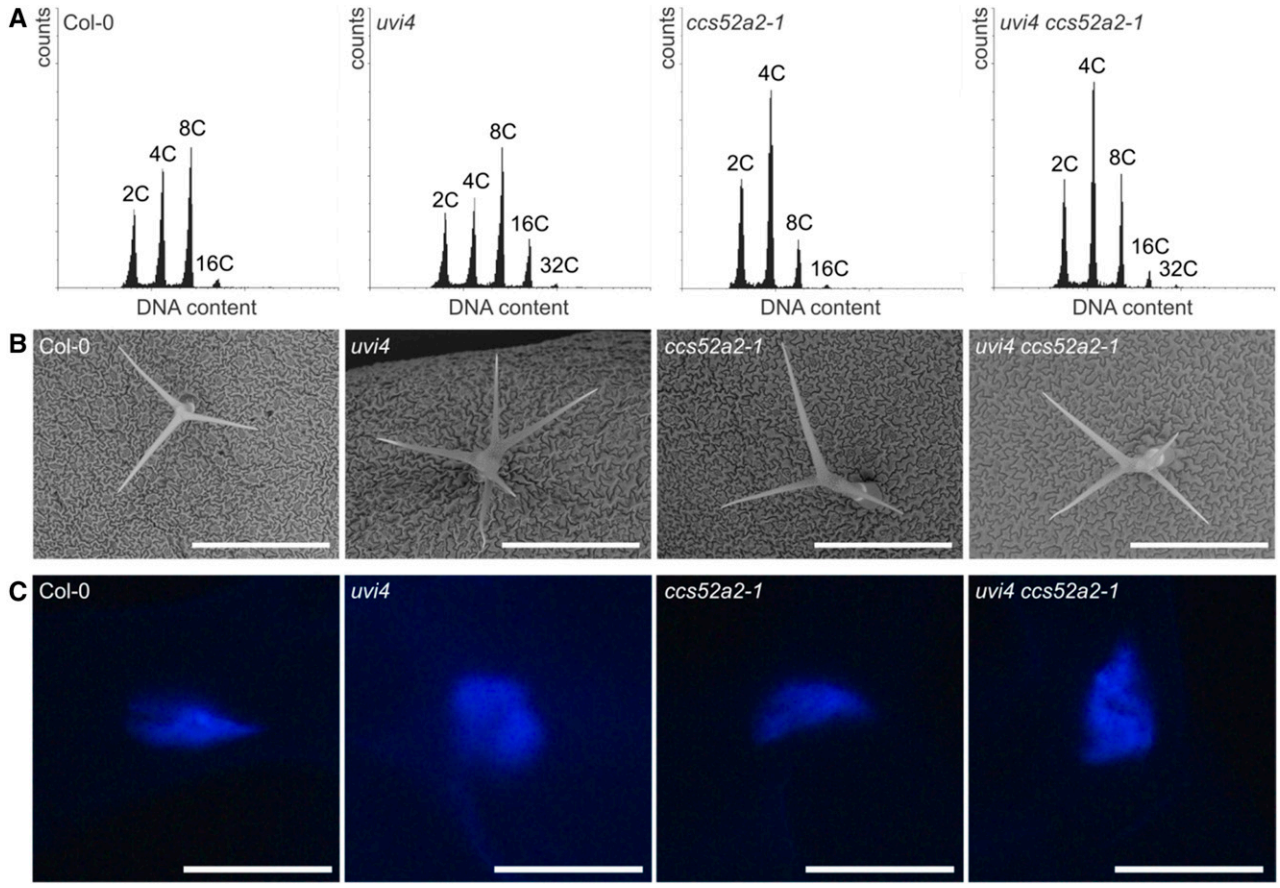

Figure 2. Endoreplication phenotypes of the *uvi4 ccs52a2-1* double mutant. A, Flow cytometric analysis of wild-type (Col-0), *uvi4*, *ccs52a2-1*, and *uvi4 ccs52a2-1* three-week-old first true leaves. Data are representative for the mean ($n = 3$). B, Scanning electron microscope images of wild-type (Col-0), *uvi4*, *ccs52a2-1*, and *uvi4 ccs52a2-1* trichomes. Images are representative for the mean. Bars = 300 μm. C, Epifluorescence images of DAPI-stained wild-type, *uvi4*, *ccs52a2-1*, and *uvi4 ccs52a2-1* trichome nuclei. Images are representative for the mean ($n > 8$). Bars = 10 μm.

a role for both APC/C^{CCS52A1} and APC/C^{CCS52A2} in the development of different tissues.

UVI4 and DEL1 Contribute Independently to Trichome Development

To study the effects of a lack of both a functional *UVI4* and *DEL1*, we generated a *uvi4 del1-1* double mutant, which is anticipated to result in an increased activity of both APC/C^{CCS52A1} and APC/C^{CCS52A2} complexes. Similar to the *uvi4* mutant, *del1-1* mutants were found to display an increased trichome branching phenotype (Fig. 3C; Supplemental Fig. S3S). Correspondingly, quantification of the trichome nuclear size revealed an increase in the DNA content in *del1-1* mutant trichomes, similar to the *uvi4* mutant, indicative for a role of DEL1 in suppressing endoreplication in trichomes (Fig. 3D; Supplemental Fig. S3B). In the *uvi4 del1-1* double mutant, a clearly enhanced effect on trichome branching could be observed (Fig. 3C; Supplemental Fig. S3A), with a correspondingly increased trichome nuclear size compared to the single mutants (Fig. 3D; Supplemental Fig. S3B). These data suggest that both UVI4 and DEL1, and hence APC/C^{CCS52A1} and APC/C^{CCS52A2}, control trichome branching.

UVI4 and DEL1 Independently Regulate Root Meristem Size Maintenance

In the Arabidopsis root, *CCS52A1* expression can be found in the root elongation zone, where it controls the timing of cell cycle exit. Accordingly, mutation of *UVI4* results in a decreased root meristem size, reflected by a decrease in the number of meristematic cortex cells, probably owing to an increased APC/C^{CCS52A1} activity (Heyman et al., 2011). On the other hand, *CCS52A2* expression can be found predominantly in the QC cells, where it is required to keep these cells from dividing and differentiating (Vanstraelen et al., 2009). Because the DEL1 transcriptional repressor of *CCS52A2* is expressed throughout the root meristem, it was tested whether *DEL1* mutation affects root meristem size maintenance.

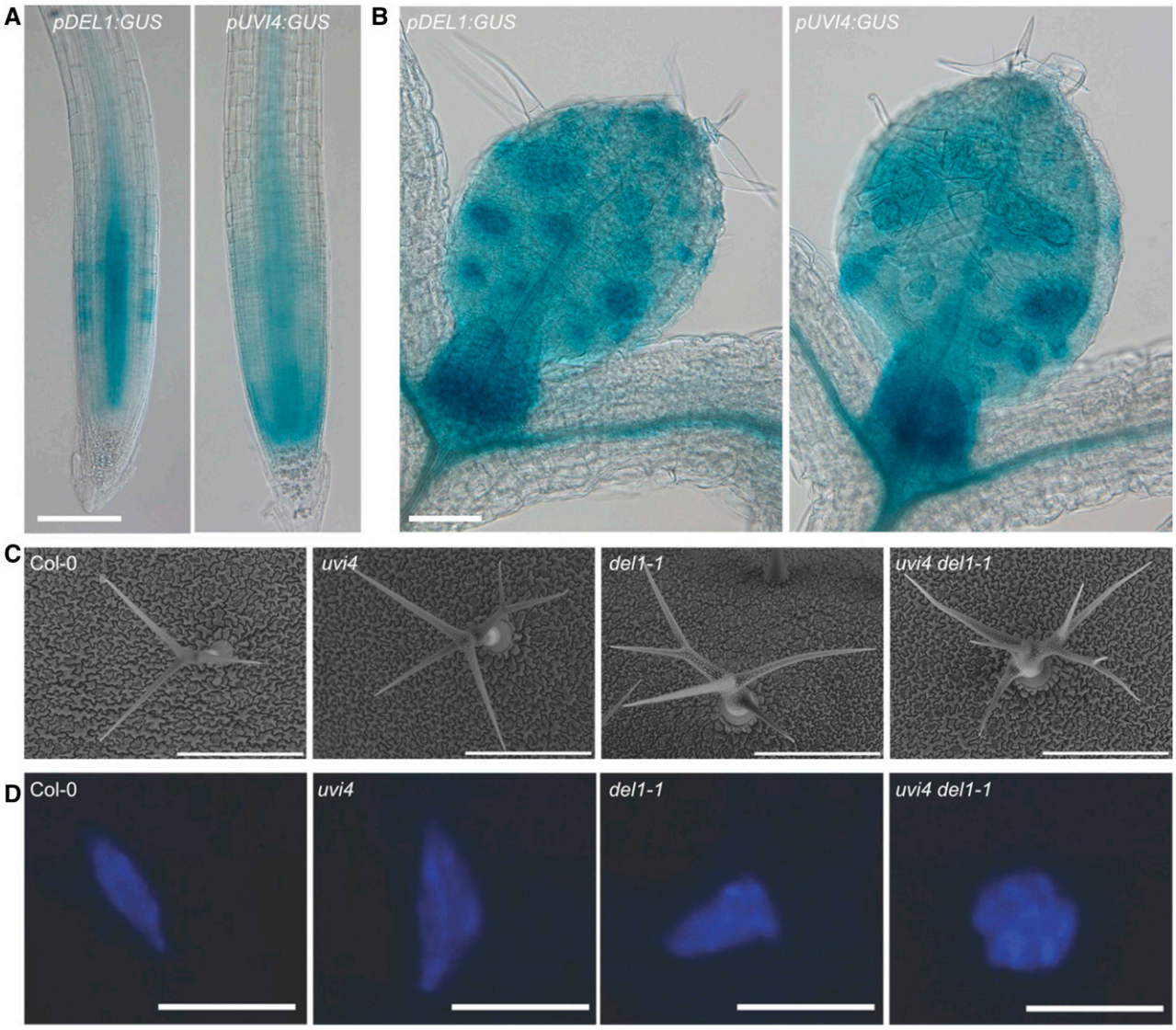

Figure 3. UVI4 and DEL1 independently control trichome ploidy levels. A and B, Expression pattern of *UVI4* and *DEL1* in the root meristem (A) and leaves (B). Bars = 0.1 mm. C, Scanning electron microscope images of wild-type (Col-0), *uvi4*, *del1-1*, and *uvi4 del-1* trichomes. Images are representative for the mean. Bars = 300 μm. D, Epifluorescence images of DAPI-stained wild-type, *uvi4*, *del-1*, and *uvi4 del-1* trichome nuclei. Images are representative for the mean ($n > 8$). Bars = 10 μm.

No significant decrease in the number of meristematic cortex cells could be observed in the *del1-1* mutant compared to wild-type roots (Fig. 4, A and B). In contrast, when determining the root meristem size of the *uvi4 del1-1* double mutant, a significant reduction in the number of meristematic cortex cells could be observed compared to both the *uvi4* and *del1-1* single mutants (Fig. 4, A and B). This reduction was offset by an increased cortex cell size, resulting in a meristem size similar to that of the wild type.

When determining the DNA ploidy levels of *uvi4* and *del1-1* mutant roots, an increase could be observed for both compared to those of wild-type roots (Fig. 4C; Supplemental Table S3). When determining the DNA ploidy levels of *uvi4 del1-1* double mutant roots, an increase could be detected compared to the single *uvi4* and *del1-1* mutants (Fig. 4C; Supplemental Table S3). These observations suggest that both APC/$C^{CCS52A1}$ and APC/$C^{CCS52A2}$ contribute to the DNA ploidy levels of roots.

UVI4 and DEL1 Control the Onset of Endoreplication in Leaves through a Common Mechanism

Next to the effect of the *uvi4 de11-1* double mutation in trichomes and roots, we tested its effect on leaf development by analyzing the size of mature first true leaves. Both the *uvi4* and *del1-1* single mutants displayed a reduced leaf size compared to wild-type leaves (Fig. 5, A and B). The *uvi4 del1-1* double mutant displayed an additive effect on

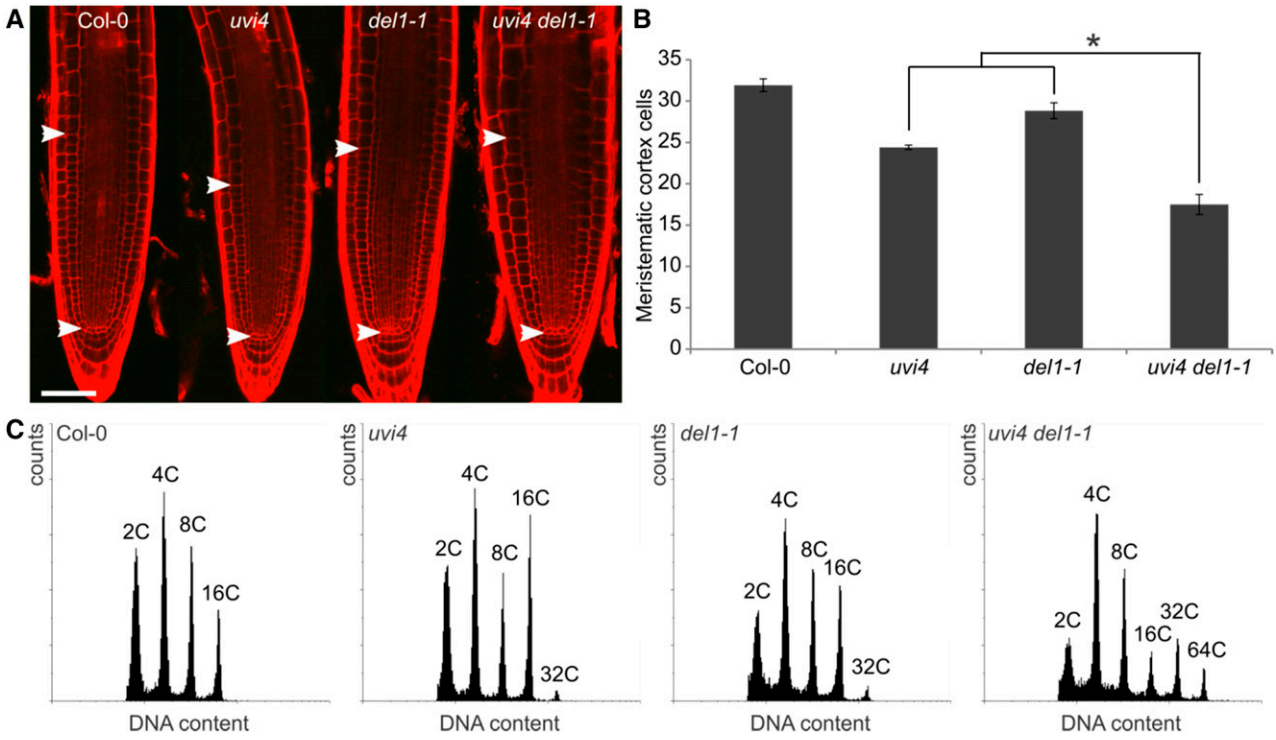

Figure 4. UVI4 and DEL1 independently control cell cycle exit in the root. A, Representative confocal microscopy images of wild-type (Col-0), *uvi4*, *del1-1*, and *uvi4 del1-1* one-week-old root meristems stained with propidium iodide. Arrowheads indicate the meristem size based on the cortical cell length. Bar = 50 μm. B, Number of meristematic cortex cells for lines presented in (A). Data represent mean ± SE ($n > 8$, $^*P < 0.05$, Student's *t* test). C, Flow cytometric analysis of wild-type (Col-0), *uvi4*, *del1-1*, and *uvi4 del1-1* one-week-old mutant roots. Data are representative for the mean.

the significantly reduced leaf size compared to both *uvi4* and *del1-1* single mutants (Fig. 5, A and B). To determine the cause of the reduced leaf size, the average abaxial epidermal cell number and size were investigated. The *uvi4* and *del1-1* single mutants' reduced leaf size was caused by a reduction in cell number, despite the small increase in cell size, compared to wild-type plants (Fig. 5, C and D). The *uvi4 del1-1* double mutant displayed a decrease in epidermal cell number, being equal to that seen for the single mutants, but without compensatory increase in cell size (Fig. 5, C and D). These data show that the apparent additive effect of *uvi4* and *del1* mutations on leaf size in the double mutant is not caused by the additive effects of the single mutations on epidermal cell size and cell number.

Seeing how double mutation of *UVI4* and *DEL1* has strong additive effects on the DNA ploidy levels in trichomes and roots, we tested whether a similar additive effect could hold true for leaves. When determining the DNA ploidy levels of mature leaves in the *uvi4* and *del1-1* single mutants, an increase could be confirmed compared to wild-type plants (Vlieghe et al., 2005; Heyman et al., 2011; Fig. 5E; Supplemental Table S4). However, the DNA ploidy distributions of the *uvi4 del1-1* double mutant leaves did not differ significantly from the *uvi4* and *del1-1* single mutants (Fig. 5E; Supplemental Fig. S4; Supplemental Table S4), which is in contrast to the results obtained in trichomes and roots, suggesting that APC/$C^{CCS52A1}$ and APC/$C^{CCS52A2}$ are interdependent in the leaf.

CCS52A2 Expression Is Affected by CCS52A1 Activity

The observation that the DNA ploidy levels of the *uvi4 del1-1* double mutant leaves are similar to those of the single mutants, is contradicting the gene dosage effect observed in *ccs52a1-1 DEL1*^{OE} mutants. To investigate this apparent paradox, we analyzed the *CCS52A* expression levels in developing first true leaves of the *uvi4*, *del1-1*, and *uvi4 del1-1* mutants using RT-qPCR. To ensure the seedlings were at a similar developmental age, leaves were harvested at stage 1.04 (Boyes et al., 2001). For *CCS52A1*, no major differences in expression could be observed in the mutants compared to the wild type (Fig. 6A). By contrast, when determining the *CCS52A2* transcript levels in the *del1-1* mutant, an up-regulation could be observed, confirming previous data (Lammens et al., 2008; Fig. 6A). Surprisingly, mutation of *UVI4* also resulted in an increased *CCS52A2* expression in first true leaves compared to wild-type leaves (Fig. 6A), suggesting that activation of APC/$C^{CCS52A1}$ results in increased *CCS52A2* expression. In the *uvi4 del1-1* double mutant stage 1.04 leaves, however, no

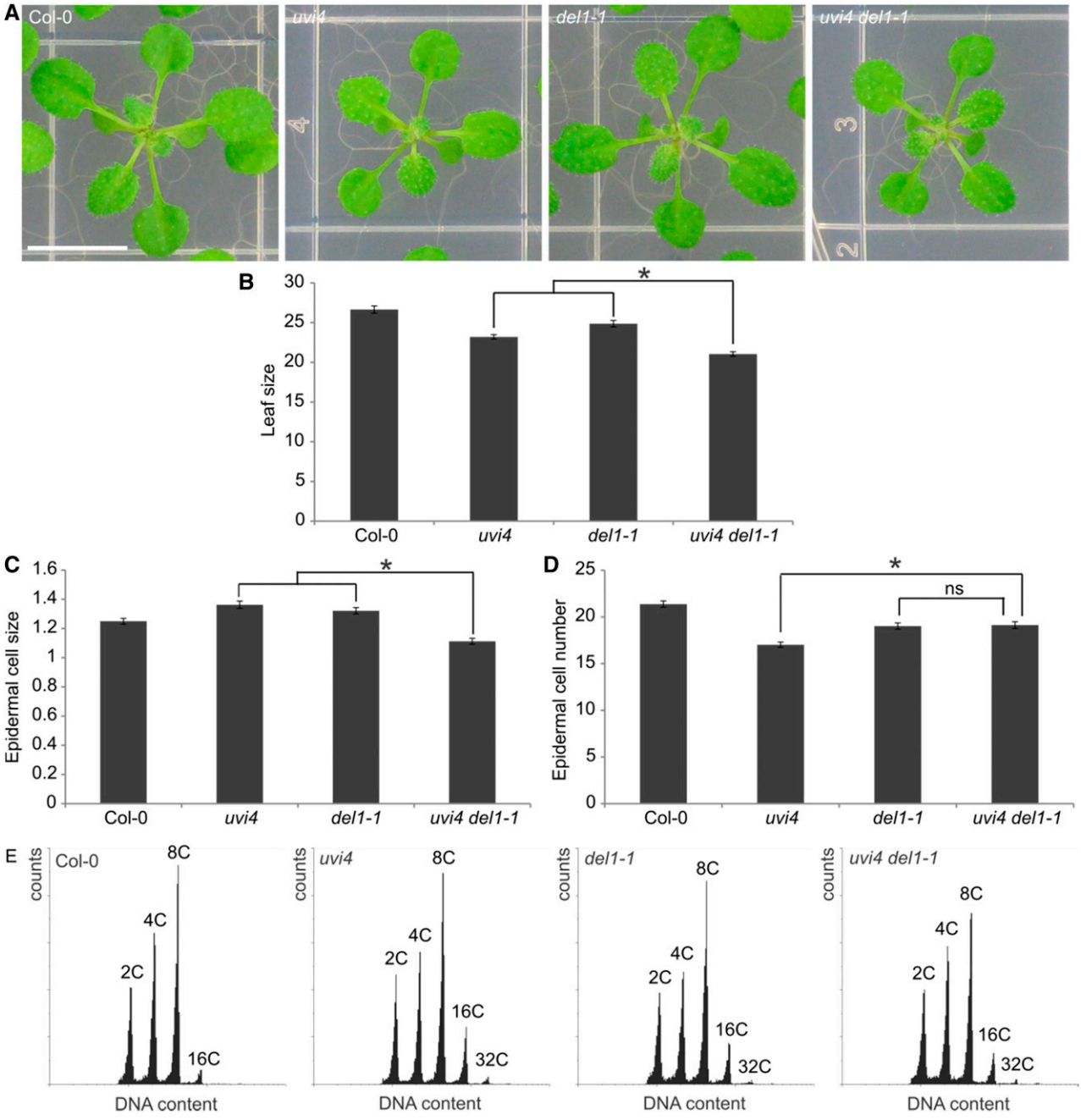

Figure 5. UVI4 and DEL1 control leaf ploidy levels through a common mechanism. A, Images of three-week-old wild-type (Col-0), *uvi4*, *del1-1*, and *uvi4 del1-1* rosettes. Bar = 1 cm. B, Average first true leaf sizes of three-week-old wild-type (Col-0), *uvi4*, *del1-1*, and *uvi4 del1-1* plants (in mm^2). Data represent mean ± SE ($n = 45$, $*P < 0.05$, Student's *t* test). C and D, Average abaxial epidermal cell size (× 1.000 μm^2) and average cell number (× 1.000), respectively, of first leaves of three-week-old lines presented in (B). Data represent mean ± SE ($n = 18$, $*P < 0.05$, Student's *t* test). E, Flow cytometric analysis of wild-type (Col-0), *uvi4*, *del1-1*, and *uvi4 del1-1* three-week-old first true leaves. Data are representative for the mean ($n = 3$).

additive effect on *CCS52A2* expression could be observed, as *CCS52A2* transcript levels were found to be increased, identical to those observed in the *del1-1* mutant (Fig. 6A).

To confirm that an increase in APC/$C^{CCS52A1}$ activity results in transcriptional activation of *CCS52A2*, *CCS52A2* transcript levels were analyzed in wild-type versus *CCS52A1*^{OE} leaves harvested at stage 1.04. Indeed, *CCS52A2* transcript levels were increased in *CCS52A1*^{OE} leaves, similar to *uvi4* mutant leaves (Fig. 6B), suggesting that increased APC/$C^{CCS52A1}$ activity results in increased *CCS52A2* expression.

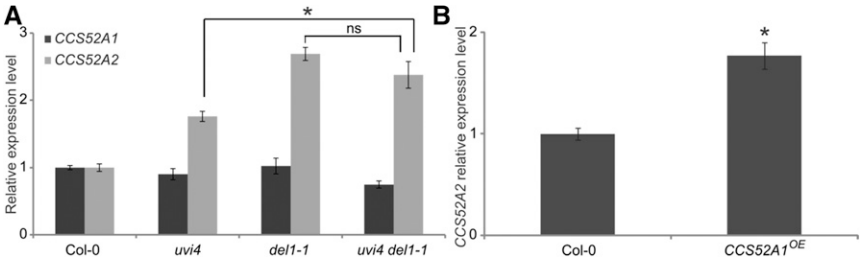

Figure 6. CCS52A1 activity affects *CCS52A2* expression. A, Relative expression levels of *CCS52A1* and *CCS52A2* in first true leaves from wild-type (Col-0), *uvi4*, *del1-1*, and *uvi4 del1-1*. First true leaves were harvested at stage 1.04. The relative expression levels for wild-type leaves were arbitrarily set to 1. Data represent mean ± SE ($n = 3$, $^*P < 0.05$, Student's *t* test). B, Increased *CCS52A2* transcript levels in $CCS52A1^{OE}$ first true leaves compared to the wild type. First true leaves were harvested at stage 1.04. The relative expression levels for wild-type leaves were arbitrarily set to 1. Data represent mean ± SE ($n = 3$, $^*P < 0.05$, Student's *t* test).

DISCUSSION

(Non)Redundant Functions of CCS52A1 and CCS52A2

Both APC/C activity-controlling proteins CCS52A1 and CCS52A2 play important functions during plant development. CCS52A1 has been predominantly implicated in controlling trichome branching and root ploidy levels (Vanstraelen et al., 2009; Kasili et al., 2010), whereas CCS52A2 has been demonstrated to control the proliferation status of the root QC stem cells (Vanstraelen et al., 2009) and shoot apical meristem maintenance (Liu et al., 2012). Although CCS52A1 and CCS52A2 control different developmental processes, functional redundancy is expected, as plants being deficient for both *CCS52A* genes are not viable (Baloban et al., 2013). Indeed, endoreplication onset in leaves is ensured by both CCS52A-type proteins. Furthermore, during plant growth, a decreased expression of *CCS52A1* appears to be compensated by an increased expression of *CCS52A2* (Baloban et al., 2013). To overcome the problem of lethality, we generated a partial loss-of-function mutant using the *ccs52a1-1* $DEL1^{OE}$ double mutant in which the absence of *CCS52A1* is accompanied with reduced *CCS52A2* transcription owing to its increased repression by DEL1 (Lammens et al., 2008). Whereas no clear obvious additive effects could be observed in the development of tissues that are predominantly controlled by CCS52A1, being the trichomes or the root meristem, the leaf DNA ploidy levels were further decreased in the *ccs52a1-1* $DEL1^{OE}$ double mutant compared to the single mutants. Therefore, it could be stated that some tissues are more dependent on the *CCS52A* gene redundancy compared to others.

UVI4 and DEL1 Specifically Fine-Tune APC/C^{CCS52A} Activity

The *uvi4 ccs52a2-1* double mutant displays a trichome branching and DNA ploidy phenotype being intermediate to that observed for the single *uvi4* and *ccs52a2-1* mutants, which is in contrast to the observation that the *ccs52a1-1* mutation is epistatic over the *uvi4* mutation (Heyman et al., 2011). Together with the previously observed lack of protein-protein interactions between UVI4 and CCS52A2, these observations support the idea that UVI4 is a specific inhibitor of the APC/$C^{CCS52A1}$ complex. How such specificity might be achieved at the protein level is unclear. The CCS52A1 and CCS52A2 proteins share a high sequence homology, including the C-box, Cdh1 specific motif, cyclin-binding, and C-terminal IR motif, together with predicted CDK phosphorylation sites (Fülöp et al., 2005). Extending our knowledge of CCS52A structural domains might help shed light on the preference of the UVI4 protein inhibitor.

The specificity of DEL1 toward regulating *CCS52A2* expression was demonstrated previously by specific binding of DEL1 to the *CCS52A2* promoter and exclusive changes in *CCS52A2* transcription levels in $DEL1^{OE}$ and *del1-1* knockout lines (Lammens et al., 2008). Whereas these observations were made for complete seedling and leaf tissue, respectively, a control of *CCS52A2* expression by DEL1 can be observed as well for root tissue (Supplemental Fig. S6, A and B), strongly suggesting that DEL1 is a specific repressor of *CCS52A2* across all *DEL1* expressing cells.

Additive Effects of *UVI4* and *DEL1*

The specificity of UVI4 and DEL1 toward APC/$C^{CCS52A1}$ and APC/$C^{CCS52A2}$, respectively, offers a unique tool to study the relative contribution of both APC/C complexes during development, complementing available knockout data. This strategy has as benefit that the APC/C activity levels obtained remain within a physiological range, in contrast to constitutive *CCS52A1* or *CCS52A2* overexpression, where it can be expected that complexes lose substrate specificity when being highly abundant. Using this strategy, we revealed an additive effect of *uvi4* and *del1* knockout on trichome branching and ploidy level, indicating that DEL1 functions to actively repress APC/$C^{CCS52A2}$ activity in trichome cells. Accordingly, ectopic expression of *CCS52A2* triggers trichome hyperbranching (Baloban et al., 2013). A similar situation likely holds true for the root, as *uvi4 del1-1* double knockouts display a phenotypic enhancement of the *uvi4* and

del1-1 single knockouts, again suggesting that DEL1 plays an active role in suppressing APC/$C^{CCS52A2}$ activity in the meristematic cells, supported by the *DEL1* expression pattern. Apparently contrasting with an APC/$C^{CCS52A2}$-repressing role for DEL1, *del1-1* single mutant roots are phenotypically indistinguishable from wild-type roots in terms of meristem size. These data suggest that APC/$C^{CCS52A1}$ is the primary APC/C complex controlling cell cycle exit in the root elongation zone (Vanstraelen et al., 2009). Strikingly, the aggravated meristematic cell number phenotype of *del1-1* in the *uvi4* mutant background was accompanied by an increased meristematic cortex cell size, suggesting an increased cell cycle duration. Knowing that APC/$C^{CCS52A2}$ activity represses cell division activity of the QC cells, it is appealing to speculate that transcriptional activation of *CCS52A2* throughout the root meristem here also delays cell cycle progression, resulting in the observed increased cell size.

Cross Talk between APC/$C^{CCS52A1}$ and APC/$C^{CCS52A2}$ Activity

Contrary to trichomes and root meristems, where APC/$C^{CCS52A1}$ activity predominantly controls endoreplication onset, in the leaf, both CCS52A1 and CCS52A2 control the DNA ploidy level (Lammens et al., 2008; Baloban et al., 2013). Correspondingly, mutation of *UVI4* or *DEL1* results in leaves containing increased DNA ploidy levels, likely due to increased APC/$C^{CCS52A1}$ or APC/$C^{CCS52A2}$ activity, respectively. Surprisingly, no additive effect on the leaf DNA ploidy levels could be detected upon *UVI4* and *DEL1* double mutation. Rather, the double mutant results suggest a linear pathway. Strikingly, increased APC/$C^{CCS52A1}$ activity was found to boost *CCS52A2* expression. Here, the effect of CCS52A1 on *CCS52A2* expression might be DEL1-dependent, because the increased *CCS52A2* transcript level in the *uvi4 del1-1* double mutant leaves appeared to be similar to that of *del1-1* single mutant leaves. How DEL1 activity could be controlled by APC/$C^{CCS52A1}$ remains unknown. In mammalian systems, atypical E2F proteins are recognized by APC/C^{CDH1} through a KEN-box motif and are subsequently marked for proteolytic degradation (Boekhout et al., 2016). However, no obvious APC/C recognition degron can be found in the DEL1 protein sequence. Another possibility is that DEL1 activity is regulated through its phosphorylation, because a predicted CDK phosphorylation motif is present in the N terminus of the DEL1 protein sequence (Supplemental Fig. S5; Chang et al., 2007). Increased APC/$C^{CCS52A1}$-mediated destruction of cyclins could reduce putative CDK-mediated phosphorylation of DEL1, possibly rendering it unable to repress *CCS52A2* expression. Although nothing is known about the regulation of DEL proteins through phosphorylation, DEL1 has been shown to interact with CYCB2;3 and CYCD1;1 in a yeast two-hybrid screen, hinting to a connection between DEL1 and the cyclin-CDK machinery (Boruc et al., 2010).

Another possible explanation might be that, in leaves, activation of APC/$C^{CCS52A1}$ or APC/$C^{CCS25A2}$ alone is sufficient to surpass a specific activity threshold to engage into the endocycle, e.g. through destruction of a factor being rate limiting for endocycle onset. This hypothesis would imply that CCS52A1 and CCS52A2 only control leaf endocycle onset, and not endocycle progression itself. Correspondingly, in trichomes, APC/C^{CCS52} activity has been postulated to mediate endoreplication onset, whereas following endocycles are thought to be maintained by the CULLIN4-RING FINGER-LIGASE ubiquitin ligase (Roodbarkelari et al., 2010). A similar endocycle onset/maintenance mechanism might hold true for leaves as well. In this scenario, the additive effects of *UVI4* and *DEL1* mutations observed in root meristems and trichomes would be suggestive for CCS52A1- and CCS52A2-independent functions, e.g. through different substrate specificity.

In conclusion, gaining more insight into the tissue-specific substrates and substrate specificity of APC/$C^{CCS52A1}$ and APC/$C^{CCS52A2}$ will strongly contribute to the understanding of how APC/C-dependent endocycle onset is fine-tuned during development. In the root, CYCA2;3 has been reported to be a specific target of APC/$C^{CCS52A1}$ in the root elongation zone (Boudolf et al., 2009), whereas the ERF115 transcription factor was proposed to be a APC/$C^{CCS52A2}$-specific target in root stem cells (Heyman et al., 2013). A possible method to uncover specific APC/C substrates is by using a biochemical approach. A proteomics screen to identify differentially ubiquitinated proteins (Walton et al., 2016) in the *ccs52a1* and *ccs52a2* mutants might prove a major step forward. Alternatively, mutant suppressor screens could be adverted to search for APC/$C^{CCS52A1}$ or APC/$C^{CCS52A2}$ specific targets. Finding the answer to these questions might shed light on why certain tissues predominantly advert only one of the two CCS52A proteins, whereas other organs depend on both CCS52A-type isoforms.

MATERIALS AND METHODS

Plant Medium and Growth Conditions

Arabidopsis thaliana wild type and mutants are in the Columbia-0 (Col-0) background. Plants were grown under a long-day/short-night regime (16-h light/8-h darkness) at 21°C on agar-solidified culture medium (Murashige & Skoog medium, 10 g/L saccharose, 0.43 g/L MES, and 0.8% [w/v] plant tissue culture agar).

Mutant Lines

The *uvi4* (Hase et al., 2006), *pUVI4:GUS/GFP* (Heyman et al., 2011), *pDEL1:GUS/GFP*, *ccs52a1-1* and *ccs52a2-1* (Lammens et al., 2008), *del1-1* and $DEL1^{OE}$ (Vlieghe et al., 2005), and $CCS52A1^{OE}$ (Vanstraelen et al., 2009) mutants and reporter lines used have been described previously. Double mutants were generated by crossing and validated by genotyping.

Flow Cytometry Analysis

Leaves were chopped with a razor blade in 200 μL CyStain UV Precise nuclei extraction buffer (Partec) and DNA was stained by adding 800 μL staining

buffer (Partec). Nuclei were measured with CyFlow Flow Cytometer (Partec) and analyzed with the CXP Analysis software (Partec). Three or more leaves originating from different plants were analyzed for each technical repeat. The endoreduplication index was calculated as follows: $EI = [(0 \times \%2C \text{ nuclei}) + (1 \times \%4C \text{ nuclei}) + (2 \times \%8C \text{ nuclei}) + (3 \times \%16C \text{ nuclei}) + (4 \times \%32C \text{ nuclei})]$.

Leaf and Cellular Parameter Determination

Mature first true leaves were harvested and cleared using a 75:25 (v/v) ethanol/acetic acid solution. Next, leaves were fixed and mounted on a slide using lactic acid. Cells were drawn using a DF microscope (Leica). Analysis of the leaf area was performed using the software ImageJ 1.41 (National Institutes of Health).

Quantification of Trichome Nuclear DNA Content

For 4′,6-diamidino-2-phenylindole (DAPI) staining, 3-week-old mature leaves were fixed using acetic acid (75:25 [v/v] acetic acid/ethanol) for at least 2 h and washed for at least 1 h with 70% (v/v) ethanol. Leaves were briefly submerged in 0.5 M EDTA and trichomes were removed using forceps. DNA was stained using 20 μg/mL DAPI in McIlvaine's buffer (60 mM citric acid, 80 mM Na_2HPO_4, pH 4.1). Trichomes were mounted in Vectashield mounting medium (No. CA94010; Vector Laboratories) for fluorescence H1000 (Vector Laboratories) and observed via epifluorescence on an Axioscope Imager microscope (Zeiss). Nuclear size and epifluorescence signal were analyzed using the software ImageJ 1.41. The integrated density was calculated by multiplication of nuclear size and fluorescence intensity, normalized against the integrated density of wild-type Col-0 trichome nuclei, of which the size was arbitrarily set to 32C.

Confocal and Scanning Electron Microscopy

Root meristems were analyzed with Axiovert 100M confocal laser scanning microscopy (Zeiss). Plant material was incubated for 3 min in a 10-μM propidium iodide solution to stain the cell walls and observed after excitation using a 543-nm laser and detected using the 650-nm long-pass emission filter. Images of leaf trichomes were acquired with a TM-1000 Tabletop electron microscope (Hitachi).

RT-qPCR Analysis

RNA was extracted from the respective tissues with the RNeasy Kit (Qiagen). After treatment with the RQ1 RNase-Free DNase (Promega), cDNA was synthesized using the iScript cDNA Synthesis Kit (Bio-Rad). Relative expression levels were determined with the LightCycler 480 Real-Time SYBR green PCR System (Roche). The *ACT* and *CAK2* reference genes were used for normalization. Primer sequences can be found in Supplemental Table S5.

Accession Numbers

Sequence data from this article can be found in the Arabidopsis Genome Initiative or GenBank/EMBL databases under the following accession numbers: *CCS52A1* (At4G22910); *CCS52A2* (At4G11920); *DEL1* (At3G48160); *UVI4* (At2G42260)

Supplemental Data

The following supplemental materials are available.

Supplemental Figure S1. Quantification of wild-type (Col-0), *ccs52a1-1*, *DEL1^{OE}*, and *ccs52a1-1 DEL1^{OE}* trichome branch number and nuclear DNA content.

Supplemental Figure S2. Quantification of wild-type (Col-0) and *uvi4*, *ccs52a2-1*, and *uvi4 ccs52a2-1* trichome branch number and nuclear DNA content.

Supplemental Figure S3. Quantification of wild-type (Col-0) and *uvi4*, *del1-1*, and *uvi4 del1-1* mutant trichome branch number and nuclear DNA content.

Supplemental Figure S4. Endoreduplication index of wild-type (Col-0), *uvi4*, *del1-1*, and *uvi4 del1-1* mature leaves reveals no significant difference in leaf ploidy distributions of the *uvi4 del1-1* double mutant compared to the *uvi4* and *del1-1* single mutants.

Supplemental Figure S5. Putative CDK phosphorylation site in the DEL1 N-terminal sequence.

Supplemental Figure S6. *CCS52A1* and *CCS52A2* expression levels in *del1-1* and *DEL1^{OE}* mutant leaves and roots.

Supplemental Table S1. DNA ploidy distribution of three-week-old first true leaves of wild-type (Col-0), *ccs52a1-1*, *DEL1^{OE}*, and *ccs52a1-1 DEL1^{OE}* plants.

Supplemental Table S2. DNA ploidy distribution of three-week-old mature first true leaves of the wild-type (Col-0), *uvi4*, *ccs52a2-1*, and *uvi4 ccs52a2-1* plants.

Supplemental Table S3. DNA ploidy distribution of one-week-old roots of the wild-type (Col-0), *uvi4*, *del1-1*, and *uvi4 del1-1* plants.

Supplemental Table S4. DNA ploidy distribution of three-week-old first true leaves of wild-type (Col-0), *uvi4*, *del1-1*, and *uvi4 del1-1* plants.

Supplemental Table S5. List of primers used for RT-qPCR analysis.

ACKNOWLEDGMENTS

The authors thank Annick Bleys for help in preparing the manuscript.

Received June 12, 2017; accepted July 7, 2017; published July 11, 2017.

LITERATURE CITED

Baker DJ, Dawlaty MM, Galardy P, Van Deursen JM (2007) Mitotic regulation of the anaphase-promoting complex. Cell Mol Life Sci **64:** 589–600

Baloban M, Vanstraelen M, Tarayre S, Reuzeau C, Cultrone A, Mergaert P, Kondorosi E (2013) Complementary and dose-dependent action of AtCCS52A isoforms in endoreduplication and plant size control. New Phytol **198:** 1049–1059

Beemster GT, De Vusser K, de Tavernier E, De Bock K, Inzé D (2002) Variation in growth rate between Arabidopsis ecotypes is correlated with cell division and A-type cyclin-dependent kinase activity. Plant Physiol **129:** 854–864

Beemster GTS, Vercruysse S, De Veylder L, Kuiper M, Inzé D (2006) The *Arabidopsis* leaf as a model system for investigating the role of cell cycle regulation in organ growth. J Plant Res **119:** 43–50

Boekhout M, Yuan R, Wondergem AP, Segeren HA, Van Liere EA, Awol N, Jansen I, Wolthuis RMF, De Bruin A, Westendorp B (2016) Feedback regulation between atypical E2Fs and APC/C^{Cdh1} coordinates cell cycle progression. EMBO Rep **17:** 414–427

Boruc J, Van Den Daele H, Hollunder J, Rombauts S, Mylle E, Hilson P, Inzé D, De Veylder L, Russinova E (2010) Functional modules in the *Arabidopsis* core cell cycle binary protein-protein interaction network. Plant Cell **22:** 1264–1280

Boudolf V, Lammens T, Boruc J, Van Leene J, Van Den Daele H, Maes S, Van Isterdael G, Russinova E, Kondorosi E, Witters E, De Jaeger G, Inzé D, et al (2009) CDKB1;1 forms a functional complex with CYCA2;3 to suppress endocycle onset. Plant Physiol **150:** 1482–1493

Bourdon M, Pirrello J, Cheniclet C, Coriton O, Bourge M, Brown S, Moïse A, Peypelut M, Rouyère V, Renaudin J-P, Chevalier C, Frangne N (2012) Evidence for karyoplasmic homeostasis during endoreduplication and a ploidy-dependent increase in gene transcription during tomato fruit growth. Development **139:** 3817–3826

Boyes DC, Zayed AM, Ascenzi R, McCaskill AJ, Hoffman NE, Davis KR, Görlach J (2001) Growth stage-based phenotypic analysis of Arabidopsis: a model for high throughput functional genomics in plants. Plant Cell **13:** 1499–1510

Bramsiepe J, Wester K, Weinl C, Roodbarkelari F, Kasili R, Larkin JC, Hülskamp M, Schnittger A (2010) Endoreplication controls cell fate maintenance. PLoS Genet **6:** e1000996

Breuer C, Ishida T, Sugimoto K (2010) Developmental control of endocycles and cell growth in plants. Curr Opin Plant Biol **13:** 654–660

Breuer C, Morohashi K, Kawamura A, Takahashi N, Ishida T, Umeda M, Grotewold E, Sugimoto K (2012) Transcriptional repression of the APC/C activator CCS52A1 promotes active termination of cell growth. EMBO J **31:** 4488–4501

Cebolla A, Vinardell JM, Kiss E, Oláh B, Roudier F, Kondorosi A, Kondorosi E (1999) The mitotic inhibitor ccs52 is required for endoreduplication and ploidy-dependent cell enlargement in plants. EMBO J **18:** 4476–4484

Chang EJ, Begum R, Chait BT, Gaasterland T (2007) Prediction of cyclin-dependent kinase phosphorylation substrates. PLoS One **2:** e656

De Veylder L, Larkin JC, Schnittger A (2011) Molecular control and function of endoreplication in development and physiology. Trends Plant Sci **16:** 624–634

Edgar BA, Zielke N, Gutierrez C (2014) Endocycles: a recurrent evolutionary innovation for post-mitotic cell growth. Nat Rev Mol Cell Biol **15:** 197–210

Flemming AJ, Shen Z-Z, Cunha A, Emmons SW, Leroi AM (2000) Somatic polyploidization and cellular proliferation drive body size evolution in nematodes. Proc Natl Acad Sci USA **97:** 5285–5290

Fülöp K, Tarayre S, Kelemen Z, Horváth G, Kevei Z, Nikovics K, Bakó L, Brown S, Kondorosi A, Kondorosi E (2005) Arabidopsis anaphase-promoting complexes: multiple activators and wide range of substrates might keep APC perpetually busy. Cell Cycle **4:** 1084–1092

Hamdoun S, Zhang C, Gill M, Kumar N, Churchman M, Larkin JC, Kwon A, Lu H (2016) Differential roles of two homologous cyclin-dependent kinase inhibitor genes in regulating cell cycle and innate immunity in Arabidopsis. Plant Physiol **170:** 515–527

Hase Y, Trung KH, Matsunaga T, Tanaka A (2006) A mutation in the *uvi4* gene promotes progression of endo-reduplication and confers increased tolerance towards ultraviolet B light. Plant J **46:** 317–326

Heyman J, Cools T, Vandenbussche F, Heyndrickx KS, Van Leene J, Vercauteren I, Vanderauwera S, Vandepoele K, De Jaeger G, Van Der Straeten D, De Veylder L (2013) ERF115 controls root quiescent center cell division and stem cell replenishment. Science **342:** 860–863

Heyman J, De Veylder L (2012) The anaphase-promoting complex/cyclosome in control of plant development. Mol Plant **5:** 1182–1194

Heyman J, Van Den Daele H, De Wit K, Boudolf V, Berckmans B, Verkest A, Alvim Kamei CL, De Jaeger G, Koncz C, De Veylder L (2011) *Arabidopsis* ULTRAVIOLET-B-INSENSITIVE4 maintains cell division activity by temporal inhibition of the anaphase-promoting complex/cyclosome. Plant Cell **23:** 4394–4410

Imai KK, Ohashi Y, Tsuge T, Yoshizumi T, Matsui M, Oka A, Aoyama T (2006) The A-type cyclin CYCA2;3 is a key regulator of ploidy levels in *Arabidopsis* endoreduplication. Plant Cell **18:** 382–396

Kasili R, Walker JD, Simmons LA, Zhou J, De Veylder L, Larkin JC (2010) SIAMESE cooperates with the CDH1-like protein CCS52A1 to establish endoreplication in *Arabidopsis thaliana* trichomes. Genetics **185:** 257–268

Lammens T, Boudolf V, Kheibarshekan L, Zalmas LP, Gaamouche T, Maes S, Vanstraelen M, Kondorosi E, La Thangue NB, Govaerts W, Inzé D, De Veylder L (2008) Atypical E2F activity restrains APC/$C^{CCS52A2}$ function obligatory for endocycle onset. Proc Natl Acad Sci USA **105:** 14721–14726

Larkins BA, Dilkes BP, Dante RA, Coelho CM, Woo YM, Liu Y (2001) Investigating the hows and whys of DNA endoreduplication. J Exp Bot **52:** 183–192

Lilly MA, Duronio RJ (2005) New insights into cell cycle control from the *Drosophila* endocycle. Oncogene **24:** 2765–2775

Liu Y, Ye W, Li B, Zhou X, Cui Y, Running MP, Liu K (2012) CCS52A2/FZR1, a cell cycle regulator, is an essential factor for shoot apical meristem maintenance in *Arabidopsis thaliana*. BMC Plant Biol **12:** 135

Magyar Z, Horváth B, Khan S, Mohammed B, Henriques R, De Veylder L, Bakó L, Scheres B, Bögre L (2012) *Arabidopsis* E2FA stimulates proliferation and endocycle separately through RBR-bound and RBR-free complexes. EMBO J **31:** 1480–1493

Mathieu-Rivet E, Gévaudant F, Sicard A, Salar S, Do PT, Mouras A, Fernie AR, Gibon Y, Rothan C, Chevalier C, Hernould M (2010) Functional analysis of the anaphase promoting complex activator CCS52A highlights the crucial role of endo-reduplication for fruit growth in tomato. Plant J **62:** 727–741

Melaragno JE, Mehrotra B, Coleman AW (1993) Relationship between endopolyploidy and cell size in epidermal tissue of Arabidopsis. Plant Cell **5:** 1661–1668

Narbonne-Reveau K, Senger S, Pal M, Herr A, Richardson HE, Asano M, Deak P, Lilly MA (2008) APC/$C^{Fzr/Cdh1}$ promotes cell cycle progression during the *Drosophila* endocycle. Development **135:** 1451–1461

Perazza D, Herzog M, Hülskamp M, Brown S, Dorne A-M, Bonneville J-M (1999) Trichome cell growth in *Arabidopsis thaliana* can be derepressed by mutations in at least five genes. Genetics **152:** 461–476

Peters J-M (2002) The anaphase-promoting complex: proteolysis in mitosis and beyond. Mol Cell **9:** 931–943

Roodbarkelari F, Bramsiepe J, Weinl C, Marquardt S, Novák B, Jakoby MJ, Lechner E, Genschik P, Schnittger A (2010) Cullin 4-ring finger-ligase plays a key role in the control of endoreplication cycles in Arabidopsis trichomes. Proc Natl Acad Sci USA **107:** 15275–15280

Takahashi N, Kajihara T, Okamura C, Kim Y, Katagiri Y, Okushima Y, Matsunaga S, Hwang I, Umeda M (2013) Cytokinins control endocycle onset by promoting the expression of an APC/C activator in *Arabidopsis* roots. Curr Biol **23:** 1812–1817

Vanstraelen M, Baloban M, Da Ines O, Cultrone A, Lammens T, Boudolf V, Brown SC, De Veylder L, Mergaert P, Kondorosi E (2009) APC/C^{CCS52A} complexes control meristem maintenance in the *Arabidopsis* root. Proc Natl Acad Sci USA **106:** 11806–11811

Vlieghe K, Boudolf V, Beemster GTS, Maes S, Magyar Z, Atanassova A, De Almeida Engler J, De Groodt R, Inzé D, De Veylder L (2005) The DP-E2F-like gene *DEL1* controls the endocycle in *Arabidopsis thaliana*. Curr Biol **15:** 59–63

Walton A, Stes E, Cybulski N, Van Bel M, Iñigo S, Durand AN, Timmerman E, Heyman J, Pauwels L, De Veylder L, Goossens A, De Smet I, et al (2016) It's time for some "site"-seeing: novel tools to monitor the ubiquitin landscape in *Arabidopsis thaliana*. Plant Cell **28:** 6–16

Xu Y, Jin W, Li N, Zhang W, Liu C, Li C, Li Y (2016) UBIQUITIN-SPECIFIC PROTEASE14 interacts with ULTRAVIOLET-B INSENSITIVE4 to regulate endoreduplication and cell and organ growth in Arabidopsis. Plant Cell **28:** 1200–1214